# DISPERSION ANALYSIS OF THE 2017 PERSIAN GULF OIL SPILL BASED ON REMOTE SENSING DATA AND NUMERICAL MODELLING

José Milton Neves de Souza Júnior<sup>1</sup>, Luís Felipe Ferreira de Mendonça<sup>2</sup>, Heverton da Silva Costa<sup>3</sup>, Rose Ane Pereira de Freitas<sup>4</sup>, Fernanda Casagrande<sup>5</sup>, Douglas da Silva Lindemann<sup>6</sup>, Rafael Afonso do Nascimento Reis<sup>7</sup>, Carlos Alessandre Domingos Lentini<sup>9</sup>, André Telles de Cunha Lima<sup>10</sup>.

1,2,3,9 Graduate Program in Geochemistry: Petroleum and Environment (POSPETRO) - UFBA, 40.170-110, Salvador, BA, Brazil

<sup>2</sup> Department of Oceanography – Geosciences Institute - UFBA, 40.170-110, Salvador, BA, Brazil

<sup>4,6</sup> Departamento of Meteorology – UFPEL, 96.160-000, Pelotas, RS, Brazil

<sup>7</sup> Department of Oceanography and Ecology – UFES, 29.075-053, Vitória, ES, Brazil

<sup>9,10</sup> Department of Earth and Environment Physics – Physics Institute - UFBA, 40.170-280, Salvador, BA, Brazil

<sup>5</sup>National Space Research Institute - INPE, 12.227-010, São José do Campos, SP, Brazil

<sup>8</sup>Management and Operational Center of the Amazon Protection System - CENSIAPM, 66.617-420, Brasilia, DF, Brazil

<sup>1,2,5</sup> Tropical Oceanography Group (GOAT)

# **ABSTRACT**

Oil spills, detected by SAR sensors as dark areas, are highly effective marine pollutants that affect the ocean surface. These spills change the water surface tension, attenuating capillary gravitational waves and causing specular reflections. We conducted a case study in the Persian Gulf (Arabian Sea to the Strait of Hormuz), where approximately 163,900 gal of crude oil spilled in March 2017. Our study examined the relationship between oil weathering processes and extracted backscatter values using zonal slices projected over SAR-detected oil spills. Internal backscatter values ranged from -22.5 to -23.5, indicating an oil chemical binding and minimal interaction with seawater. MEDSLIK-II simulations indicated increased oil solubilization and radar attenuation rates with wind, facilitating coastal dispersion. Higher backscatter at the spill edges compared to the core reflected different stages of oil weathering. These results highlight the complex dynamics of oil spills and their environmental impact on marine ecosystems.

**Key words** — Synthetic Aperture Radar (SAR), Oil Spills, Backscatter, Normalized Cross-Section, MEDSLIK.

#### 1. INTRODUCTION

The oil exploration industry is responsible for much of the introduction of hydrocarbons into coastal environments, with a significant impact on marine pollution [1]. Oil spilled at sea undergoes processes like evaporation and emulsification, which alter its chemical and physical properties [2] [3]. The detection of oil spills has become more efficient with the use of radar sensors (SAR), which identify dark spots in the water caused by oil due to the reduction in surface wave scattering [4] [5] [6].

Studies on marine oil detection using SAR imaging focus on the backscattered signal and attempt to correlate geochemical characteristics, such as density and API gravity, API gravity classifies oil based on specific gravity: above 30 is considered light, between 22 and 30 is medium, and below 22 is heavy [7]. The behavior of oil in the ocean varies depending on its chemical composition, affecting its solubility and dispersion after a spill, which results in thin patches of lighter products or aggregates of heavier oils [8].

Studies use backscatter signal analysis to track oil behavior in the ocean. This research analyzed a 2017 spill case in the Persian Gulf using Sentinel-1 radar images and the Lagrangian MEDSLIK-II model to assess oil dispersion, correlating it with geological characteristics and wind-driven dispersion

# 2. MATERIAL AND METHODS

The study used synthetic aperture radar (SAR) images from ESA's Sentinel-1 satellite, made up of the A and B satellites, equipped with 5.40 GHz C-band radar. The data was obtained from the Copernicus Open Access Hub in Single Look Complex (SLC) format, with 5x20m resolution, and acquired on March 8 and 11, 2017, during oil spills in the Persian Gulf, off the coast of Sharjah, United Arab Emirates. The data was pre-processed with SNAP software, including orbital correction, radiometric calibration and thermal noise removal, ensuring accuracy in the spatial detection of oil slicks and normalization of the backscatter signal.

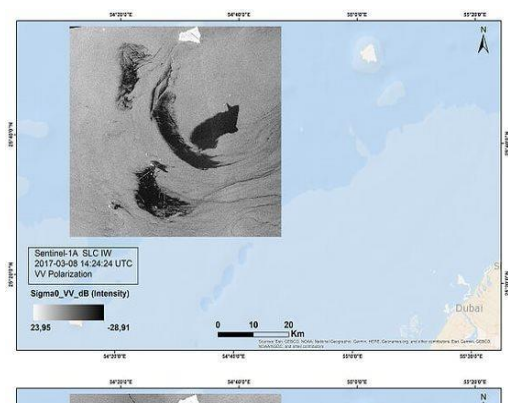
### 2.1 Extration Parameters

Backscatter values were extracted from cross-sections over identified oil slicks in two SAR images of the Persian Gulf. Sections were taken perpendicular to the slick's displacement, and backscatter values in decibels (dB) from the center and edge areas were plotted. The distinction between these areas varies with the slick's size and shape, with parameters including object standard deviation, background standard deviation, maximum contrast, and average contrast. The center-edge segregation interval was defined based on the slick's spatial arrangement, enabling the analysis of backscatter intensity variations due to oil

surface.

2844

INPE - Salvador/BA, Brasil



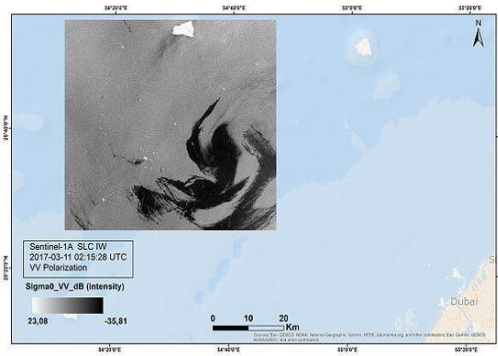


Figure 1: Sentinel-1 SAR image over the oil spill slick in the Persian Gulf on March 8 (up) and 11(down), 2017.

# 2.2 Oil slick mapping

The detection of dark areas in SAR images relies on identifying low pixel backscatter values, specifically regions with normalized radar cross-section (NRCS) less than half the average NRCS for oil slicks[9]. Dark areas in these images often have values close to the noise level of the SAR system. The average NRCS for ocean surfaces under moderate wind conditions typically ranges from -15 dB to -25 dB. SAR imaging with VV polarization offers high contrast between oil slicks and the ocean surface.

#### 2.3 Wind field analysis

Ocean surface waves are detected using microwave radar, influenced by Bragg and non-Bragg scattering mechanisms. For accurate velocity extraction in oil spills, radar backscatter attenuation is important, especially under light to moderate wind conditions that suppress Bragg waves[10]. During the Persian Gulf oil spill, average wind speeds were about 5 m/s. Wind speed extraction connects backscattered radar signals with wind characteristics, enhancing the understanding of spill dynamics.

During the Persian Gulf oil spill, average wind speeds were about 5 m/s. Wind speed extraction connects backscattered radar signals with wind characteristics, enhancing the understanding of spill dynamics. Geophysical model functions (GMFs), particularly CMOD5.N for Sentinel-1 data, estimate wind speeds using an equation that relates normalized radar cross-section (NRCS) to wind speed and direction[11].

#### 2.4 Oil Spill Model

MEDSLIK-II is a Lagrangian model described by [12][13] that uses wind, temperature, and current data to simulate oil dispersion in the seem. This model produces

aggregate oil concentrations over 150 m horizontal bins and oil mass balances at 30-minute intervals. The simulations use the JONSWAP wave spectrum as a function of wind speed[14]. The model simulates the advection-diffusion and weathering processes of oil in a discrete form, including spreading, evaporation, natural dispersion, and emulsification. MEDSLIK-II is forced with atmospheric data from ERA 5 and ocean data from CMEMS' Global Ocean Physics Reanalysis (GLORYS) and has a daily spatial resolution of 1/12o for the global ocean, with 50 vertical levels. The parameterization of MEDSLIK-II is done via source code files, and the model was run for five days starting on March 7, 2017 (table 1).

Parameters	Information
Simulation Periods	March 7-12, 2017
Duration	966h
Latitude	25.36°
Longitude	54.30°
Liters	620 liters
Oil	Sirri from Iran
Density (g/cm³)	0.871
Oil API	30.9
Temperature to determine viscosity	38
Viscosity (50°C)	7.4
Residual oil density	0.922
Residual oil percentage	57.6
Oil vapor pressure (bar)	0.650

Table 1: MEDSLIK-II simulation parameters.

# 3. RESULTS AND DISCUSSIONS

This manuscript analyzes changes in radar backscatter signals using two Sentinel-1 SAR images from an oil spill case study in the Persian Gulf. The study highlights significant alterations in the backscatter signal due to Bragg wave attenuation within 72 hours post-spill. It correlates backscatter cross-section analyses with the degradation rates of Sirri oil and examines how wind influences the dispersion and dissolution of slick patches along the UAE coast.

The first signs of oil appeared in Sentinel-1 imagery on March 8, 2017, while no changes were noted in Landsat-8 data from March 7, suggesting the oil remained in its geochemical state immediately after the spill, which was caused by drilling issues. Thermal signatures of the spill were also detected in TSM data from Metop-AVHRR.

Three cross-sections were analyzed in the March 8 SAR image, with Section 3 showing significant Bragg wave attenuation and a concave profile(figure 2). Oil solubilization occurs through physical mixing, with the baroclinic gradient forming from the slick's edges inward. The degradation of hydrocarbons is primarily facilitated by microorganisms, while the spread and dissolution depend on factors like API grade, fluid density, and local wind conditions[2]. Predominant east/southeast winds during the spill contributed to a rapid northwest spread of the slick, enhancing water

solubilization at the edges. Additionally, increased water content in the oil raised the dielectric constant, affecting backscattering observed in the sections, and indicating that wind energy can intensify capillary waves outside the slick.

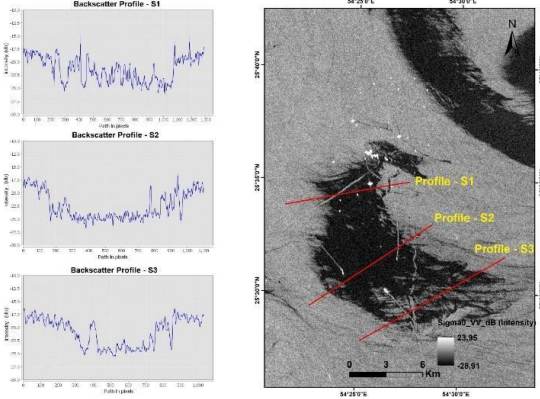


Figure 2: Cross sections for acquiring the backscatter signal response for the oil slick in the Persian Gulf on March 8, 2017.

Viscous dissipation increases with time after the start of the leakage, raising the intensity of the capillary spectrum, which plays a crucial role in propagation. An increase in NRCS values of up to 3 dB is observed in areas distant from the core, indicating homogenization of electromagnetic feedback over time. In clean ocean water, the surface tension is around 0.07 N/m, while weakly solubilized viscous substances reduce it to less than 0.040 N/m[15]. Figure 3 shows that backscatter at the stain's edge has lower values (~ -18 dB), signaling the transition between seawater and the oilcontaining region. This area indicates the degradation of hydrocarbon molecules, while the interior of the stain, with values between -22.5 and -23.5 dB, shows that the oil was still stable, with no significant interaction with seawater.

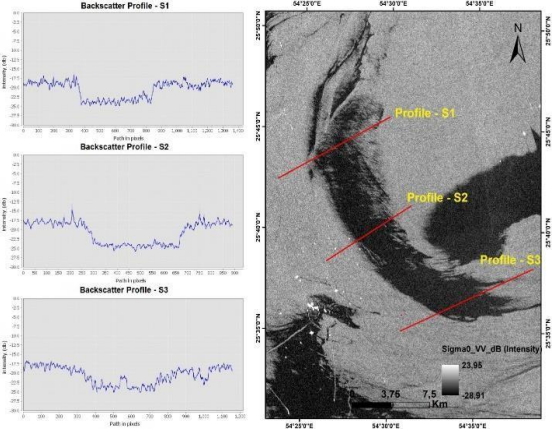


Figure 3:Cross sections for acquiring the backscatter signal response for the second portion of the oil slick on March 8.

#### Wind speed

Wind speed significantly affects the dispersion and solubilization of spilled oil, influencing radar backscatter based on the oil's density and viscosity. SAR images, using the CMOD5 algorithm, were employed to gather wind speed and direction data for spill analysis. On day 8, easterly winds averaged 2.5 m/s, with gusts over 5 m/s, while another pattern

from the east/southeast averaged 6.5 m/s, indicating decreased dispersion over the slick(figure 5). Realistic models consider both wind and surface currents to better estimate slick age. Understanding the type of oil is crucial for this estimation, as characteristics like viscosity affect slick expansion. Larger spills typically result in wider slicks, while smaller ones may create fragmented patches. Environmental conditions during SAR acquisitions were not available and might differ from simulations. Observations on day 11 revealed that backscatter was reduced within the slick but intensified at the edges and in surrounding waters.

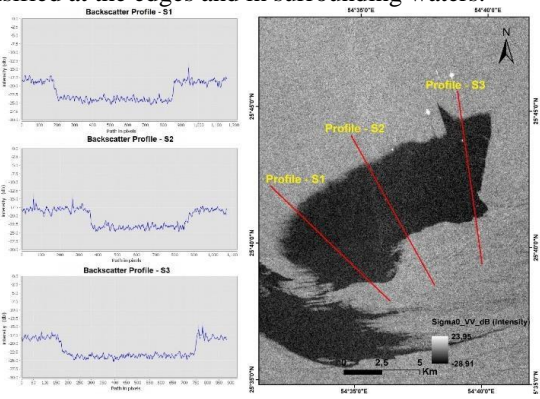


Figure 4: Cross sections for acquiring the backscattering signal response for the third oil slick on March 8.

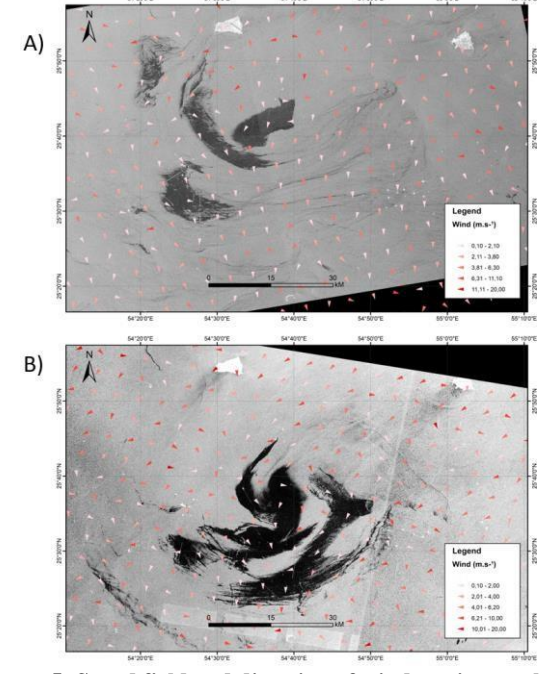


Figure 5: Speed field and direction of winds acting on the sea surface during the oil spill on March 8 (A) and 11 (B), 2017.

# MEDSLIK-II Outputs

This study used the MEDSLIK-II model to simulate the trajectory and distribution of oil during the spill, also assessing the probability of stranding in coastal areas. The model reproduced particle transport under conditions similar to those observed in SAR images, following the local

east/northeast wind pattern from day 8 onward. After the first Sentinel-1 record, the spill spread rapidly due to wind, with an increase in the oil's dielectric constant indicating higher solubilization. The simulation began on March 8, aligning with the dispersion pattern observed in the Sentinel-1 image (figure 7).

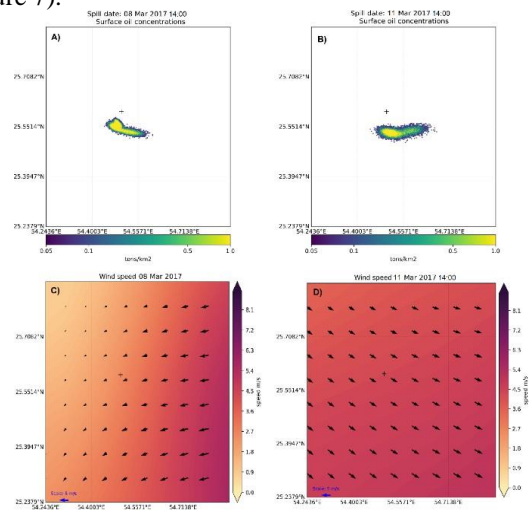


Figure 7: Persian Gulf oil spill model simulation for the two available SAR images on 03/08/2017 (Figure A) and 03/11/2017 (Figure B). The values indicate the estimated rate of oil weathering based on an initial volume of 264 gallons of spilled oil (upper panel). Wind intensity (in colors) and direction (black arrows) are displayed in the lower panel.

After ~96 hours from the start of the spill, we observe that the local wind patterns shift to the west/northwest direction, advecting the slick in an easterly direction in a longitudinal spread, as observed in the SAR image of day 11 (Figure 7D). This process also caused a latitudinal shift of the total slick volume to the south (Figure 7B). After 96 hours of numerical simulation, at 02:15 on 03/11/2017, the time of the SAR image acquisition, we observed advection and patchy separation of the spilled oil. Although this separation does not appear in our simulation, the overall dispersion pattern of the spill remains the same. Despite this, we believe that the general dispersion pattern follows the local wind direction and efficiently simulates the event.

# 4. CONCLUSIONS

Radar remote sensing is essential for understanding oil behavior on the ocean surface through backscatter values. This study shows how oil weathering, dispersion, and evaporation reduce the slick thickness and affect backscatter. Comparisons with images from the Persian Gulf revealed that wind action is crucial for oil solubilization, reducing the backscattered signal by about 1 dB every 12 hours. SAR image analysis indicated a slick at least 1 micron thick, with approximately 264 gallons of oil per square kilometer. Geochemical characteristics of the oil and environmental factors, such as wind and temperature, are equally important for horizontal dispersion. Low wind speeds reduce the contrast between water and oil, decreasing attenuation rates. This study is strategic for developing action plans against oil spills using modeling tools like MEDSLIK-II for risk assessment and supporting further investigations and automated manitoring of wilnorable areas

#### 5. REFERENCES

- [1] Fingas, M. Oil spill science and technology. Gulf professional publishing. 2016.
- [2] Alpers, W., Holt, B., & Zeng, K. Oil spill detection by imaging radars: Challenges and pitfalls. Remote sensing of environment, 201, 133-147,2017.
- [3] Chaturvedi, S. K., Banerjee, S., & Lele, S. An assessment of oil spill detection using Sentinel 1 SAR-C images. Journal of Ocean Engineering and Science, 5(2), 116-135,2020.
- [4] Abimanyu, A., Pranowo, W. S., Faizal, I., Afandi, N. K., & Purba, N. P. Reconstruction of oil spill trajectory in the Java Sea, Indonesia using sar imagery. Geography, Environment, Sustainability, 14(1), 177-184, 2021.
- [5] Marghany, M.: Automatic detection of oil spills in the Gulf of Mexico from RADARSAT-2 SAR satellite data. Environmental Earth Sciences, v. 74, n. 7, p. 5935-5947, 2015.
- [6] Migliaccio M, Nunziata F, Buono A SAR polarimetry for sea oil slick observation. Int J Remote Sens 36(12):3243–3273, 2015.
- [7] Fingas, M. Oil spill dispersants: A technical summary. In Oil spill science and technology (pp. 435-582). Gulf Professional Publishing, 2011.
- [8] Yu, J., Cao, C., & Pan, Y.Advances of adsorption and filtration techniques in separating highly viscous crude oil/water mixtures. Advanced Materials Interfaces, 8(16), 2100061, 2021.
- [9] Topouzelis, K., & Singha, S. Oil spill detection using space-borne Sentinel-1 SAR imagery. Oil Spill Science and Technology, 387-394, 2017.
- [10] Zhang, T., Li, X. M., Feng, Q., Ren, Y., & Shi, Y. Retrieval of sea surface wind speeds from Gaofen-3 full polarimetric data. Remote Sensing, 11(7), 813, 2019.
- [11] Nezhad, M. M., Groppi, D., Marzialetti, P., Fusilli, L., Laneve, G., Cumo, F., & Garcia, D. A. Wind energy potential analysis using Sentinel-1 satellite: A review and a case study on Mediterranean islands. Renewable and Sustainable Energy Reviews, 109, 499-513, 2019.
- [12] De Dominicis, M., Pinardi, N., Zodiatis, G., Lardner, R. MEDSLIK-II, a Lagrangian marinesurface oil spill model for short-term forecasting-Part 1: Theory. Geoscientific Model Development 6, 1851-1869, 2013
- [13] De Dominicis, M., Pinardi, N., Zodiatis, G., Archetti, R. MEDSLIK-II, a Lagrangian marine surface oil spill model for short-term forecasting-Part 2: Numerical simulations and validations. Geoscientific Model Development, 6, 1871-1888, 2013
- [14] Hasselmann, S., P. Lionello, and K. Hasselmann. "An optimal interpolation scheme for the assimilation of spectral wave data." Journal of Geophysical Research: Oceans 102.C7, 15823-15836, 1007.
- [15] Uzlenkov, A. V., Lutsenko, V. I., & Pavlenko, V. F. Influence of Surface-Active Substance on Angular Properties of Spectra of Signals in Centimeter-and Millimeter-Wave Bands Backscattered by Water Surface. Telecommunications and Radio Engineering, 65(1-5), 2006.